J. Plasma Physics (2004), *vol.* 70, *part* 5, *pp.* 599–611.
DOI: 10.1017/S0022377804002880 Printed in the United Kingdom

Hall dynamics and resistive tearing instability

I. F. SHAIKHISLAMOV

Department of Laser Plasmas, Institute of Laser Physics, Novosibirsk 630090, Russia
(ildar@plasma.nsk.ru)

(Received 12 March 2003 and accepted 2 January 2004)

Abstract. The stability of the neutral current sheet is analyzed in the frame of Hall dynamics. The problem is treated analytically and results are verified by numerical processing. A new version of tearing instability is found and described. It scales more favorably with the Lundquist number and has smaller wavelengths. Combined Hall magnetohydrodynamic analysis shows that Hall effects dominate the diffusion layer and growth rate of the instability in a relatively large range of sheet widths. The effect of finite beta on instability is described.

1. Introduction

The tearing instability is a well-known phenomenon that has been a subject of extensive research over the last four decades. It is believed to be important in systems with a reversed or sheared magnetic field where reconnection occurs. For the configuration of neutral current sheets, the tearing instability needs some small but finite resistivity near the neutral line. It can be supplied either by binary collisions or nonlinear collisionless processes. In the 90th space plasma observations [1] and various numerical simulations [2, 3] it was revealed that Hall effects play an important, if not crucial, role in reconnection physics. They become of consequence at a spatial scale of ion-inertia length. At these scales electrons rather than heavy ions drive the magnetic field. The most detailed analytical treatment of Hall magnetohydrodynamics (MHDs) was performed on the other widespread phenomenon common for space and laboratory plasmas, the lower hybrid drift instability [4]. Its relevance to Earth magnetotail reconnection is argued as well [5]. However, the physics of tearing and lower hybrid instabilities are quite different, especially in the geometry of the problem. The first is considered in the plane of the magnetic field while the second is perpendicular to it. Analytical investigations of Hall effects in geometries typical for reconnection problems are scanty compared to the studies based on numerical simulations. A pioneering work [6] should be mentioned, where increase of the tearing growth rate induced by Hall currents was reported for the first time. However, in this work the problem was treated mainly numerically and the analytical expression derived is only an estimation. Moreover, MHD-based dimensionless parameters that were used are not suitable for deriving explicit Hall and classic MHD limits. In [7], an analytic and numerical study of resistive reconnection revealed a strong influence of Hall currents. Incorporating Hall dynamics into global magnetic merging solutions [8] showed that it affects resistive reconnection even for sheets much thicker than the ion-inertia length.

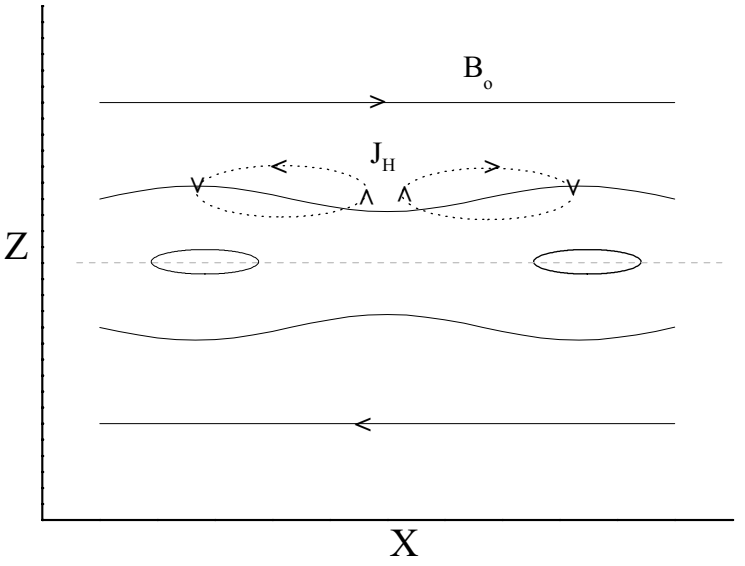

Figure 1. Geometry of the problem. Hall currents $J_{\rm H}$ that drive the reconnection are shown.

The purpose of present work is to find the new effects that Hall dynamics bring into the resistive tearing instability of relatively thin current sheets. For this, we first solve the problem in a pure electron MHD frame. In comparison to [8], such an approach gives more insight into the physics behind Hall dynamics. The problem is treated by means of classic analysis [9] and the results are verified by numerical simulation.

This paper is organized as follows. In Sec. 2 the tearing instability is described in the frame of Hall dynamics with ion motion ignored. Section 3 deals with combined Hall MHDs. In Sec. 4 the finite beta effect is considered, followed by conclusions in Sec. 5.

2. Tearing instability in the frame of Hall dynamics

We start with the generalized Ohm's law with electron mass ignored:

$$\mathbf{E} + \frac{\mathbf{v}\times\mathbf{B}}{c} = \eta\mathbf{J} - \frac{\nabla p}{ne} + \frac{\mathbf{J}\times\mathbf{B}}{nec}. \tag{1}$$

Further, the geomagnetic tail coordinate system will be used. The problem is restricted to two dimensions with $\partial/\partial y = 0$ and is schematically shown in the Fig. 1. Initial conditions for the magnetic field are

$$B_x = B_0(z/d), \quad B_y = 0, \quad B_z = 0, \tag{2}$$

where d is the characteristic width of the current sheet. We simplify the problem further by setting the temperature to be constant at all times: $T = T_{\rm i} + T_{\rm e} =$ constant. Then the term $\nabla p/ne$ in Ohm's law becomes inoperative. Using transformations $\mathbf{B}/B_0 \to \mathbf{b}$, $\mathbf{x}/d \to \mathbf{x}, t/\tau_{\rm H} \to t$, $\mathbf{v}/V_{\rm A} \to \mathbf{v}$, $n/n_0 \to n$, Hall MHD equations can be

https://doi.org/10.1017/S0022377804002880 Published online by Cambridge University Press

written in the following dimensionless form:

$$\begin{aligned}\frac{\partial n}{\partial t} &= -\chi\nabla(n\mathbf{v}),\\ \frac{\partial \mathbf{v}}{\partial t} &= -\chi\left[(\mathbf{v}\nabla)\mathbf{v} - \frac{\mathbf{j}\times\mathbf{b}}{n} - \frac{\beta}{2}\frac{\nabla n}{n}\right],\\ \frac{\partial \mathbf{b}}{\partial t} &= \chi\nabla\times(\mathbf{v}\times\mathbf{b}) - \nabla\left(\frac{\mathbf{j}\times\mathbf{b}}{n}\right) + \frac{1}{S_{\mathrm{H}}}\nabla^2 b,\\ \mathbf{j} &= \nabla\mathbf{b}.\end{aligned} \tag{3}$$

Here the following parameters were introduced:

$$\begin{aligned}\tau_{\mathrm{H}} &= 4\pi n_0 e d^2/cB_0,\\ S_{\mathrm{H}} &= 4\pi d^2/(\eta\tau_{\mathrm{H}}c^2) = \omega_{\mathrm{ce}}\tau_{\mathrm{coll}},\\ \chi &= d\cdot\omega_{\mathrm{pi}}/c.\end{aligned} \tag{4}$$

The Hall time τ_{H} is a typical time scale of Hall induced processes, while S_{H} is the analog of the Lundquist number. Note that it does not depend on characteristic size, which is also an intrinsic property of Hall dynamics. The parameter χ defines a domain where Hall effects are important—at scales smaller than ion inertia length ($d < c/\omega_{\mathrm{pi}}$). At the ion inertia scale length, the Hall time is equal to the inverse ion cyclotron frequency: $\tau_{\mathrm{H}}(d = c/\omega_{\mathrm{pi}}) = 1/\omega_{\mathrm{ci}}$. From the equations it follows that at $\chi \ll 1$ ion velocity and density evolution can be ignored. This validates the idea of analyzing pure Hall dynamics and finding the new effects it may contain, which is the main purpose of this work. Thus, in this section we only consider the vector equation of the magnetic field evolution. For small perturbations, using a property $\nabla\mathbf{b} = 0$, it can be written as equations for two components:

$$\begin{aligned}\frac{\partial b_z}{\partial t} &= -\frac{b_0}{n}\frac{\partial^2 b_y}{\partial x^2} + \frac{1}{S_{\mathrm{H}}}\nabla^2 b_z,\\ \frac{\partial b_y}{\partial t} &= \frac{b_0}{n}\nabla^2 b_z - b_z\frac{\partial}{\partial z}\left(\frac{1}{n}\frac{\partial b_0}{\partial z}\right) + \frac{1}{S_{\mathrm{H}}}\nabla^2 b_y.\end{aligned} \tag{5}$$

The component b_z causes the initially parallel magnetic field lines to curve. This curvature in turn generates the out-of-plane b_y component, which is a direct manifestation of Hall dynamics. Currents associated with the b_y component curve the in-plane magnetic field further and the cycle repeats. Let us consider wave-like perturbations with wave vector along the main magnetic field: $\sim\exp(-ik_x\cdot x)$. Then the equations reduce to a pair of one-dimensional second-order differential equations

$$\begin{aligned}\frac{\partial b_z}{\partial t} &= k^2\frac{b_0}{n}b_y + \frac{1}{S_{\mathrm{H}}}(b_z'' - k^2 b_z),\\ \frac{\partial b_y}{\partial t} &= \frac{b_0}{n}(b_z'' - k^2 b_z) - (b_0'/n)' b_z + \frac{1}{S_{\mathrm{H}}}(b_y'' - k^2 b_y).\end{aligned} \tag{6}$$

In the analytical analysis, terms of order k^2/S_{H} will be ignored as they are small and inessential. If we ignore dissipation altogether, the equations can be combined

https://doi.org/10.1017/S0022377804002880 Published online by Cambridge University Press

as

$$\frac{\partial^2 b_z}{\partial t^2} = -k^4 \left(\frac{b_0}{n}\right)^2 b_z + k^2 \left(\frac{b_0}{n}\right)^2 b_z'' - k^2 \frac{b_0}{n}(b_0'/n)' b_z. \tag{7}$$

The first two terms on the right-hand side of (7) constitute a well-known whistler wave. The third term, usually being negative for the current sheet, makes the equation potentially unstable. Instability may only be realized at sufficiently small wave numbers, because at $k \sim 1$ the whistler mode stabilizes it. One can also see that without dissipation, instability is not possible as at the origin all terms vanish. This makes it similar to the well-known resistive tearing instability, the ion velocity being replaced in this case by Hall currents. Therefore, the problem will be treated with a similar approach.

A solution will be sought in the form of a standing growing wave $\sim \exp(\gamma t)$. For the analytical treatment we shall use the current sheet of a simple step-like form: $b_0 = 1$ for $z > 1$; $b_0 = z$ for $0 \leqslant z \leqslant 1$. Because of symmetry it is sufficient to solve (6) for $z \geqslant 0$ with even b_z and odd b_y. In this section we consider the problem in the approximation of constant density $n = n_0$. For an equilibrium current sheet it corresponds to the limit of very large thermal beta $\beta \to \infty$. Although this approximation is not usually strictly applicable, it does not affect the difference between Hall and MHD dynamics because the driving term $(b_0'/n)'$ is the same in both cases. Thus, the term $(b_0'/n)'$ becomes a delta-function that is zero everywhere except $z = 1$. Because diffusion is small, it can be neglected except near the origin. Solutions are derived in three different regions: outer region $z > 1$, inner region $\delta \leqslant z \leqslant 1$ and dissipation layer $0 \leqslant z \leqslant \delta$ with some $\delta \ll 1$. At $z = 1$ they are matched by a jump condition induced by the delta function: $(b_z'/b_z)_{1-} = 1 + (b_z'/b_z)_{1+}$. At $z = \delta$ it should simply be continuous $(b_z'/b_z)_{\delta-} = (b_z'/b_z)_{\delta+}$. Equation (7) outside the diffusion layer can be written as

$$b_z'' - \left[\left(\frac{\gamma}{k} \cdot \frac{n}{b_0}\right)^2 + k^2\right] \cdot b_z = 0. \tag{8}$$

Introducing the parameter $\alpha = \gamma/k$ we may now find solutions for each region. We start with the outer region:

$$\begin{gathered} b_z'' - (\alpha^2 + k^2) \cdot b_z = 0, \\ b_z \sim \exp(-z \cdot \sqrt{\alpha^2 + k^2}). \end{gathered} \tag{9}$$

In the inner region, the solution can be expressed through a series of $k^2 z^2$:

$$b_z'' - \frac{\alpha^2 + k^2 z^2}{z^2} \cdot b_z = 0,$$

$$b_z \approx C \cdot z^{p_1} \left(1 + \frac{k^2 z^2}{(p_1+2)(p_1+1)} + \cdots\right) + z^{p_2} \left(1 + \frac{k^2 z^2}{(p_2+2)(p_2+1)} + \cdots\right),$$

$$p_{1,2} = \frac{1 \pm \sqrt{1 + 4\alpha^2}}{2}. \tag{10}$$

Because $k^2 \ll 1$, it can be simplified to $b_z \approx C \cdot z^{p_1} + z^{p_2}$. It is not continuous at the origin as $p_2 < 0$. Namely for this reason, we patch solutions at $z = \delta$ rather than calculate a jump across a singular layer, as in the classic MHD case. The constant

https://doi.org/10.1017/S0022377804002880 Published online by Cambridge University Press

C is derived from the jump condition at $z = 1$:

$$C = (p_1 - \sqrt{\alpha^2 + k^2})/(p_1 - 1 + \sqrt{\alpha^2 + k^2}). \tag{11}$$

In the dissipation layer, all terms on the right-hand side of (6) except diffusion may be ignored in the first approximation:

$$\begin{gathered} b_z'' - b_z/\gamma S_{\mathrm{H}} = 0, \\ b_z \sim \mathrm{ch}(z \cdot \sqrt{\gamma S_{\mathrm{H}}}). \end{gathered} \tag{12}$$

At $z = \delta$, from (10) and (12) one obtains

$$\begin{gathered} (b_z'/b_z)_{\delta-} = \sqrt{\gamma S_{\mathrm{H}}}\tanh(\delta\sqrt{\gamma S_{\mathrm{H}}}) \approx \gamma S_{\mathrm{H}}\delta, \\ (b_z'/b_z)_{\delta+} = \frac{1}{\delta} \cdot \frac{p_1 C\delta^{p_1} + p_2\delta^{p_2}}{C\delta^{p_1} + \delta^{p_2}}, \\ \delta^{\sqrt{1+4\alpha^2}} = \frac{(p_1 - 1 + \gamma S_{\mathrm{H}}\delta^2) \cdot (p_1 - 1 + \sqrt{\alpha^2 + k^2})}{(p_1 - \gamma S_{\mathrm{H}}\delta^2) \cdot (p_1 - \sqrt{\alpha^2 + k^2})}. \end{gathered} \tag{13}$$

To find the width of the dissipation layer, we make transformations $\bar{z} = z\sqrt{S_{\mathrm{H}}k}$, $\bar{b}_y = b_y\sqrt{k/S_{\mathrm{H}}}$. Then (6) renormalized becomes

$$\begin{gathered} \alpha b_z = \bar{z} \cdot \bar{b}_y + \partial^2 b_z/\partial\bar{z}^2, \\ \alpha\bar{b}_y = \bar{z} \cdot \partial^2 b_z/\partial\bar{z}^2 + \partial^2\bar{b}_y/\partial\bar{z}^2. \end{gathered} \tag{14}$$

In the second equation, the term proportional to k/S_{H} was ignored. From (14) it is seen that the dissipation layer is $\delta \approx 1/\sqrt{S_{\mathrm{H}}k}$. It appears that α is always small so the solution of (14) can be expanded in a series of $\bar{z}$. It should be sought in a constant b_z'', rather than constant b_z approximation (or constant ψ approximation as it is called in the literature). After substituting $b_z'' = \alpha b_z$ ($\bar{z} = 0$), a solution for $\bar{b}_y$ can be found as $\bar{b}_y \approx (b_z^0 + a) \cdot \bar{z} + a \cdot \alpha\bar{z}^3/6$. For the b_z component, it is simply $b_z \approx b_z^0 \cdot (1 + \alpha\bar{z}^2/2)$ and corresponds to (12). The constant of integration should be found from the continuity condition $(b_y'/b_y)_{\delta-} = (b_y'/b_y)_{\delta+}$ and is approximately equal to $a \approx -b_z^0(1 - \alpha/3)$; $\bar{b}_y \approx \alpha b_z^0\bar{z}/3 \cdot (1 - \bar{z}^2/2)$. After substituting $\delta = 1/\sqrt{S_{\mathrm{H}}k}$ in (13) one obtains the dispersion equation:

$$\alpha \cdot \frac{1 + \alpha}{1 - \alpha} \cdot \frac{\alpha^2 + \sqrt{\alpha^2 + k^2}}{1 + \alpha^2 - \sqrt{\alpha^2 + k^2}} = \frac{1}{\sqrt{S_{\mathrm{H}}k}}. \tag{15}$$

In (15) α^2 was neglected compared to unity whenever it does not affect the accuracy. In the limit of small wave numbers, the solution is $\gamma = (k^3/S_{\mathrm{H}})^{1/4}$. For arbitrary k the algebraic equation (15) should be solved numerically. In Fig. 2, the dependence on k is shown for the given $S_{\mathrm{H}} = 300$. As expected, there is a cut off of instability at $k \approx 1$ and a clear maximum. On the same figure, the results of the numerical time-integration of one-dimensional second-order differential equations (6) are shown. For numerical processing, a more realistic Harris current sheet with $b_0 = \tanh(z/d)$ was chosen. The problem was treated in the box $-30d \leqslant z \leqslant 30d$ with variable grid spacing and resolution near origin at least $d/1000$ or better. Further, on all figures the results of the numerical processing will be present (marked by circles) for comparison with the analytical solution. As seen from Fig. 2, the analytical solution, considering all the approximations made, is in satisfactory

https://doi.org/10.1017/S0022377804002880 Published online by Cambridge University Press

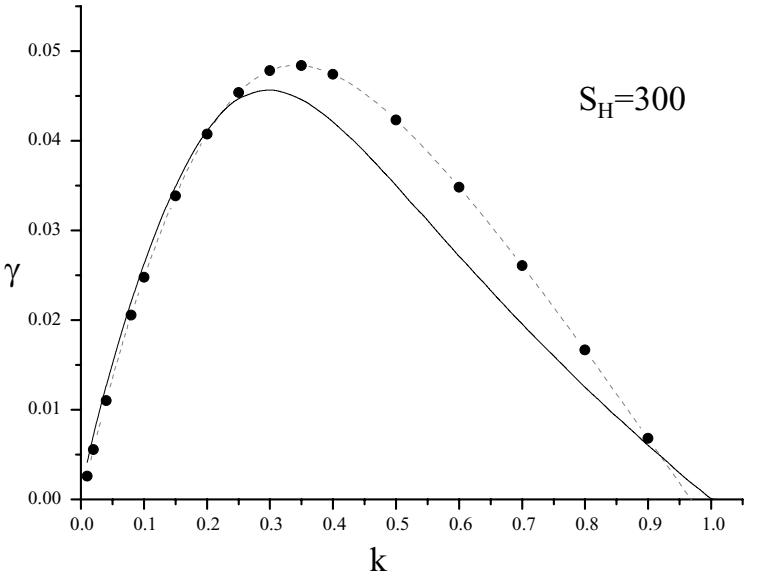

Figure 2. Dependence of the increment on wave number at Lundquist number $S_{\rm H} = 300$. The solid curve is for analytical solution, the circles represent results of numerical processing.

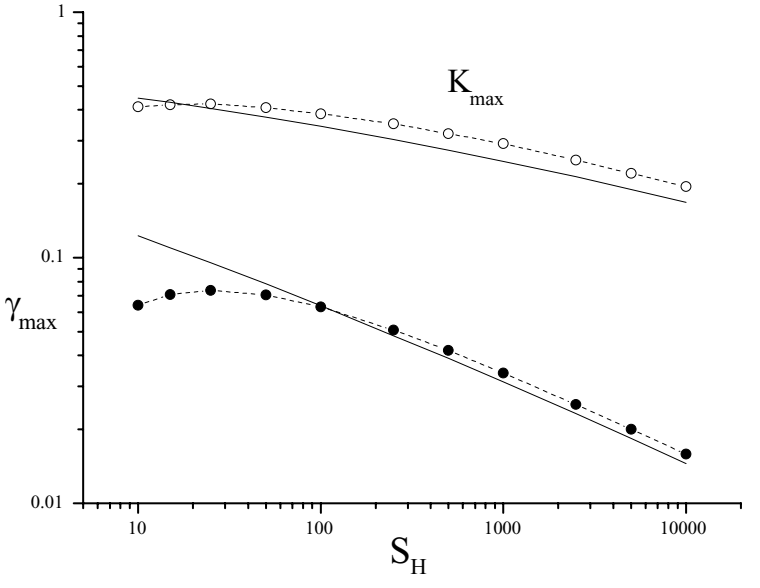

Figure 3. Maximum increment and corresponding wave number dependence on Lundquist number. Results of the numerical solution are shown by circles.

agreement with the exact numerical solution. In Fig. 3, the dependences of the maximum increment and corresponding wave number on the Lundquist number $S_{\rm H}$ are shown. Once again there is a good agreement in increment at sufficiently large $S_{\rm H}$. At moderate $S_{\rm H}$ the analytical solution breaks because the diffusion layer

https://doi.org/10.1017/S0022377804002880 Published online by Cambridge University Press

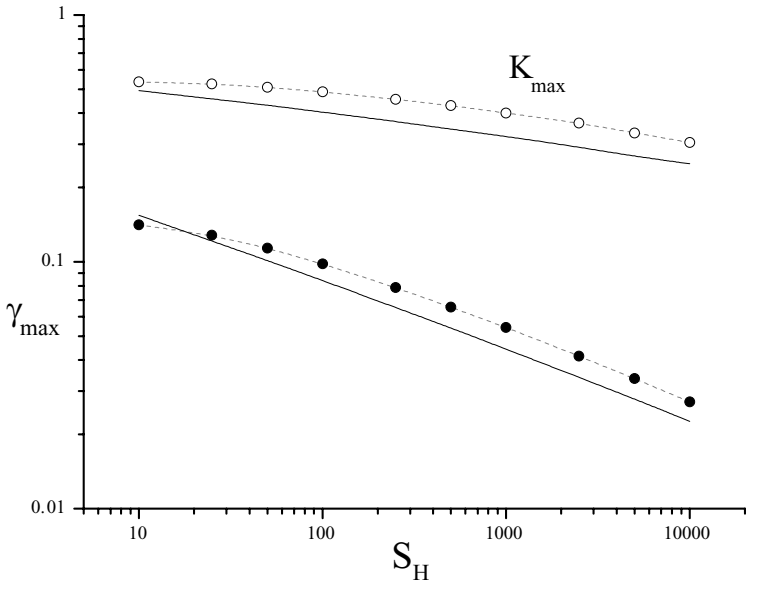

Figure 4. Maximum increment and corresponding wave number dependence on Lundquist number for the case of anisotropic resistivity.

becomes comparable with the sheet width. An approximate solution of (15) can be presented as $\gamma_{\max} \approx 1/(3 \cdot \sqrt[3]{S_{\rm H}})$ at $k_{\max} \approx 3/(4S_{\rm H}^{1/6})$.

Let us now consider the special case of anisotropic resistivity. It is physically possible that due to micro-turbulence or nonlinear processes excited by the existing current, the resistivity in the y-direction is much stronger than in others. For the tearing instability, only dissipation in the y-direction is necessary, while resistivity to the in-plane Hall currents reduces it. Without the term $b_y''/S_{\rm H}$, (6) combines to

$$b_z'' - \frac{\alpha^2 + k^2 z^2}{z^2 + \gamma/S_{\rm H} k^2} \cdot b_z = 0. \tag{16}$$

It follows that in this case the width of the diffusion layer is $\delta = \sqrt{\gamma/S_{\rm H} k^2}$. Repeating the procedure, one obtains the following dispersion relation:

$$2\alpha^{3/2} \cdot \frac{\alpha^2 + \sqrt{\alpha^2 + k^2}}{1 + \alpha^2 - \sqrt{\alpha^2 + k^2}} = \sqrt{\frac{1}{S_{\rm H} k}}. \tag{17}$$

At small k it simplifies to $\gamma = (k^4/4S_{\rm H})^{1/5}$. At large $k\,\alpha^{3/2} \approx (1-k)/(k\sqrt{4S_{\rm H}k})$ and the maximum increment approximately equals

$$\gamma_{\max} \approx \frac{(1 - k_{\max})^{2/3}}{\sqrt[3]{4S_{\rm H}}}$$

with a quite slow scaling of $k_{\max} \approx (4S_{\rm H})^{-1/8}$. In Fig. 4, the dependence of the maximum increment on Lundquist number is shown. The discrepancy between the analytical and numerical solutions is about 20% and the scaling of $\gamma_{\max}$ at large $S_{\rm H}$ is identical. It may be concluded that anisotropic resistivity increases the increment by a factor ∼2.

https://doi.org/10.1017/S0022377804002880 Published online by Cambridge University Press

3. Combined Hall MHD analysis

Let us compare the Hall induced resistive tearing instability described above with the classic MHD one, which we call the ion-tearing instability. Its maximum increment taken from [9] can be represented in the dimensionless terms used in this work as $\gamma_{\rm ion} \approx 0.6 \cdot \sqrt{\chi/S_{\rm H}}$. In general, Hall increment scales more favorably with Lundquist number as well as with the sheet width when it is smaller than $c/\omega_{\rm pi}$. The main features of the combined Hall MHD tearing instability can be understood even without solving equations, especially if conclusions are supported by numerical simulation. As was pointed out in [6], Hall dynamics couple shear Alfvén waves to the ion tearing mode because the current component J_z makes the force in the y-direction non-zero. Introducing variables $v_y = v_y\chi/(i \cdot k)$ and $v_z = v_z\chi/(i \cdot k)$, linearized equations (3) follow as

$$\begin{gathered}
\frac{\partial b_z}{\partial t} = -k^2 b_0 v_z + k^2 b_0 b_y + \frac{b_z''}{S_{\rm H}}, \\
\frac{\partial b_y}{\partial t} = b_0(b_z'' - k^2 b_z) - b_0'' b_z + b_0 k^2 v_y + \frac{b_y''}{S_{\rm H}}, \\
\frac{\partial}{\partial t}(v_z'' - k^2 v_z) = \chi^2(b_0(b_z'' - k^2 b_z t) - b_0'' b_z), \\
\frac{\partial}{\partial t} v_y = -\chi^2 b_0 b_y,
\end{gathered} \tag{18}$$

and differ from that used in [6] only in the definition of the terms.

First of all, let us consider outer and inner regions. The classic MHD solution follows from the approximation of the third equation as $b_z'' - k^2 b_z - (b_0''/b_0) \cdot b_z \approx 0$, which corresponds to the limit of large sheet width $\chi \to \infty$. It is $b_z \sim \exp(-k \cdot z)$ in the outer region and $b_z \sim 1 + z/k$ in the inner region (in the limit of small k). For Hall dynamics, because at the maximum increment it always holds that $\gamma_{\max}/k_{\max} \ll k_{\max}$, the solution is approximately the same in the outer region. In the inner region, the solution (10) is also similar since $p_2 \ll 1$, $p_1 \approx 1$, $C \approx 1/k$. Moreover, which is more important, the jump across the singular layer $\Delta' = 2/k$ is approximately equal to the corresponding value of the Hall solution $2 \cdot (b_z'/b_z)_{z=\delta}$ as well. Now let us consider how shear Alfvén wave might effect the solution. Introducing $f = b_z'' - k^2 b_z - (b_0''/b_0) \cdot b_z$ and the operator $D = \partial^2/\partial z^2 - k^2$, (18) can be combined to obtain

$$\alpha^2 D[b_z/b_0] = D\left[\frac{b_0}{1 + b_0^2\chi^2/\alpha^2} f\right] - \chi^2 b_0 f. \tag{19}$$

From (19) it is clear that with increasing χ, ion dynamics (second term on the right-hand side) become as important as Hall dynamics at relatively small $\chi \sim \sqrt{\alpha} < 1$. This is because Alfvén wave loading reduces the amplitude of Hall currents. However, at any χ the term on the left-hand side is always significantly smaller than one of the terms on the right-hand side and, in the first approximation, the solution $f \approx 0$ holds. Therefore, the only new significant addition of Hall dynamics concerns the diffusion layer, which is of crucial importance to the tearing instability anyway.

In terms of new variables $\bar{z} = z\sqrt{S_{\rm H}k^2/\gamma}$, $\bar{v}_z = v_z/\sqrt{S_{\rm H}k}$ which correspond to the diffusion layer $\delta_{\rm Hall} = \sqrt{\gamma/S_{\rm H}k^2}$ obtained previously in anisotropic resistivity case,

https://doi.org/10.1017/S0022377804002880 Published online by Cambridge University Press

(18) can be rewritten as

$$\alpha^2 b_z = -\bar{z}\cdot\bar{v}_z + (\bar{z}^2/(1+\bar{z}^2\chi^2/\gamma S_{\rm H})+1)\cdot\partial^2 b_z/\partial\bar{z}^2,$$
$$\partial^2\bar{v}_z/\partial\bar{z}^2 = (\chi\delta_{\rm Hall})^2\cdot\bar{z}\cdot\partial^2 b_z/\partial\bar{z}^2. \tag{20}$$

One can see that ion motion (namely the shear Alfvén wave) can only affect the size of diffusion layer at quite large current sheet widths $\chi > \sqrt{\gamma S_{\rm H}} \sim 0.8\cdot S_{\rm H}^{1/3} \gg 1$. In the intermediate range $\sqrt{\gamma S_{\rm H}} < \chi < \sqrt{k^2 S_{\rm H}/\gamma}$ the diffusion layer is $\delta \approx \gamma/k\chi$. At larger χ one retains, of course, the ion dominated diffusion layer $\delta^4 \cong \gamma/(k^2 S_{\rm H}\chi^2) = (\delta_{\rm Hall}/\chi)^2$. Therefore, Hall dynamics manifests itself first of all by altering the diffusion layer and dominates tearing instability in the range $\chi < S_{\rm H}^{1/3}$. This is demonstrated in Figs 5(a) and 5(b) where the maximum increment and wave number are shown as functions of sheet width $\chi = d\cdot\omega_{\rm pi}/c$ for two Lundquist numbers. Data were obtained by solving (18) numerically for the Harris sheet profile. Note that the absolute value of the growth rate is equal to $\omega_{\rm ci}(\gamma/\chi^2)$. One can see a smooth transition from the Hall to the ion-dominated region that occurs at larger χ for larger $S_{\rm H}$. The reason for the small decrease of increment in between is the additional loading by the shear Alfvén wave. Another notable feature is that in the Hall-dominated range, the maximum wave number is substantially larger and scales differently than in classic MHD case. At isotropic resistivity, the condition of the Hall-dominated diffusion layer is $\chi < \sqrt{\gamma^2 S_{\rm H}/k} \sim 0.4\cdot S_{\rm H}^{1/3}$; that is, twice lower. This case is demonstrated in Fig. 5(c). It is clear that the inclusion of Hall dynamics greatly enhances the resistive tearing instability at $\chi \leqslant 1$. For example, the classic increment at $S_{\rm H} = 10^4$ and $\chi = 1$ is approximately five times smaller than the Hall increment at anisotropic resistivity.

The reason why, even at $\chi > 1$, Hall dynamics greatly influence the diffusion layer of the tearing instability while outside it the magnetic field is driven mainly by ions, can be understood in more general physical terms. For slow incompressible motion, ion velocity is related to electron (or current) velocity as $\nabla\times\nabla\times\mathbf{v}_{\rm i} = \mathbf{v}_{\rm e}(\omega_{\rm pi}/c)^2$. Thus, close to the neutral line where $v_{{\rm i}z}, v_{{\rm e}z} \to 0$ it may be estimated $v_{{\rm i}z} \sim v_{{\rm e}z}(\delta\cdot\omega_{\rm pi}/c)^2 \ll v_{{\rm e}z}$ as long as sheet width is not too large compared with ion inertia length. In Fig. 6 the structure of the instability is shown. Hall current velocity $v_{{\rm e}z}$ and components of ion velocity $v_{{\rm i}z}$, $v_{{\rm i}y}$ are presented in the same dimensionless units. The interpretation offered in [6] that Hall dynamics increases increment due to the appearance of an intermediate layer is clearly seen. Indeed, Hall currents, as well as shear Alfvén waves, are restricted by a more compact region near the origin than the ion velocity. However, this interpretation should be completed by a statement that because of this intermediate layer, the diffusion region becomes smaller and, thus, the increment is larger.

4. Finite beta case

The case of finite beta is of practical importance to space plasma sheets. Because of the general purpose of this work, it will be considered here only in the frame of Hall dynamics. Equilibrium density is expressed in terms of beta as

$$n = 1 - b_0^2/\beta, \quad \beta = 8\pi n_0 T/B_0^2. \tag{21}$$

At $\beta \to 1$, one retrieves the original Harris sheet with zero density outside $n_\infty = 0$. Some general conclusions can be drawn from (6). It is evident that instability

https://doi.org/10.1017/S0022377804002880 Published online by Cambridge University Press

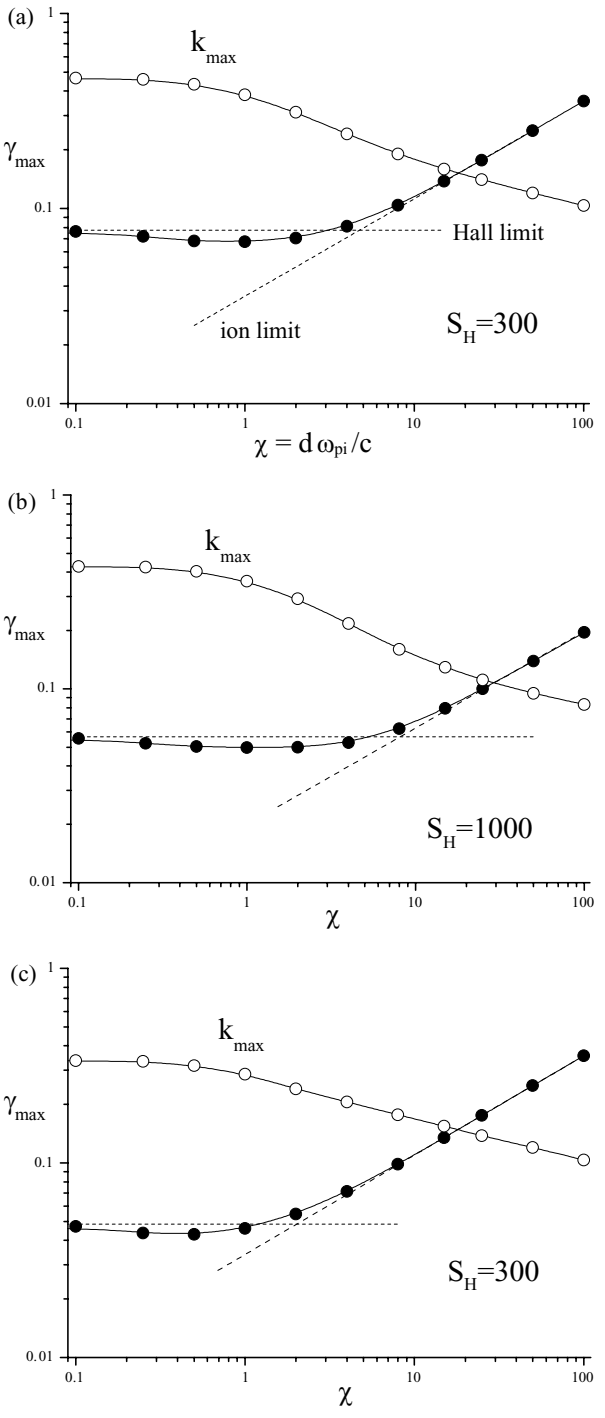

Figure 5. Dependences of the maximum increment and corresponding wave number on the current sheet width at Lundquist numbers (a) $S_H = 300$ and (b) $S_H = 1000$ for the case of anisotropic resistivity and (c) at $S_H = 300$ for isotropic resistivity. The dashed lines show solutions at small χ (Hall limit) and large χ (ion limit).

https://doi.org/10.1017/S0022377804002880 Published online by Cambridge University Press

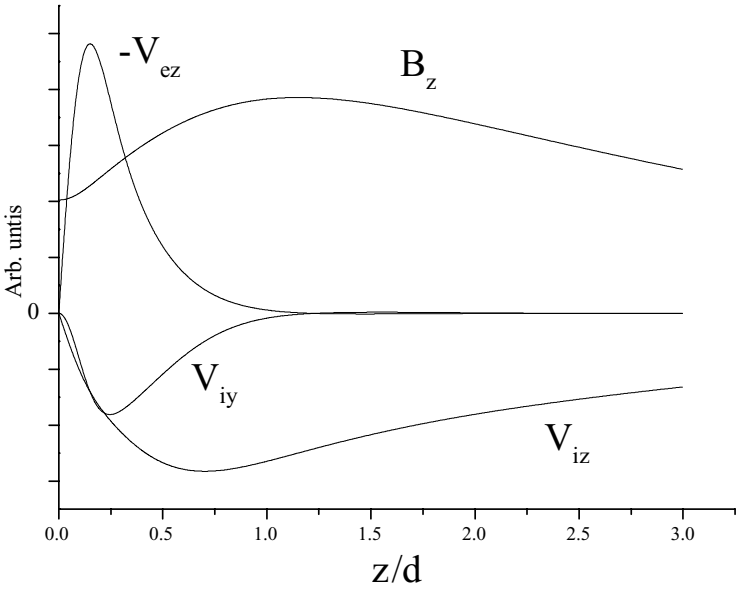

Figure 6. Typical structure of the tearing mode at $\chi = 1$.

increment should decrease simply because the driving force b_0'/n, being proportional to the relative electron–ion velocity, becomes smaller. For example, for the Harris sheet profile it can be written that $(b_0'/n)' = (b_0''/n) \cdot \nu$, $\nu = (\beta - 1)/(\beta - b_0^2) \to 0$ at $\beta \to 1$. Also, as density variation near the origin is very small, it does not affect the width of the dissipation layer. Moreover, the actual dependence $n(z)$ is of minor significance to solutions in either the outer or inner regions because it enters (8) in combination $(n\gamma/k)^2$ which is small, as was argued in the previous section. Thus, density variation may only be important at the transition between outer and inner regions. This is seen from the behavior of ν which, at $\beta \approx 1$, becomes small everywhere except at $b_0 = 1$.

At arbitrary β, (6) becomes much more complicated. To derive simple analytical expressions we employ the following trick. Use of an exact equilibrium profile of density is not necessary for the tearing instability. Instead, we adopt the step-like functions $n = n_{1+}$ at $z > 1$ and $n = n_{1-}$ at $z < 1$, and express it through the step-like function b_0' : $n = n_{1+} - (n_{1+} - n_{1-}) \cdot b_0'$. Then we calculate discontinuity ν at $z = 1$:

$$\nu = \Delta(b_z') = \int_{1-}^{1+} dz \cdot n \cdot (b_0'/n)' = \Delta(b_0') - \int_{1-}^{1+} \frac{db_0'}{n} = \frac{n_{1+}}{n_{1-} - n_{1+}} \ln\left(\frac{n_{1-}}{n_{1+}}\right). \quad (22)$$

As n_{1+} is the density, far from the origin $n_{1+} = 1 - 1/\beta$ should be taken, while in the inner region it appears best to take the averaged one: $n_{1-} = \int_0^1 dz \cdot (1 - z^2/\beta) = 1 - 1/3\beta$. Then the discontinuity can be expressed as

$$\nu = \frac{3}{2}(\beta - 1) \cdot \ln\left(\frac{\beta - 1/3}{\beta - 1}\right). \quad (23)$$

Thus, in this approximate approach, everything remains the same as in the large β case except the patching at $z = 1$: $(b_z'/b_z)_{1-} = \nu + (b_z'/b_z)_{1+}$. Note that right limits have been kept: $\nu(\infty) = 1$ and $\nu(1) = 0$. Repeating this procedure, one obtains, for

https://doi.org/10.1017/S0022377804002880 Published online by Cambridge University Press

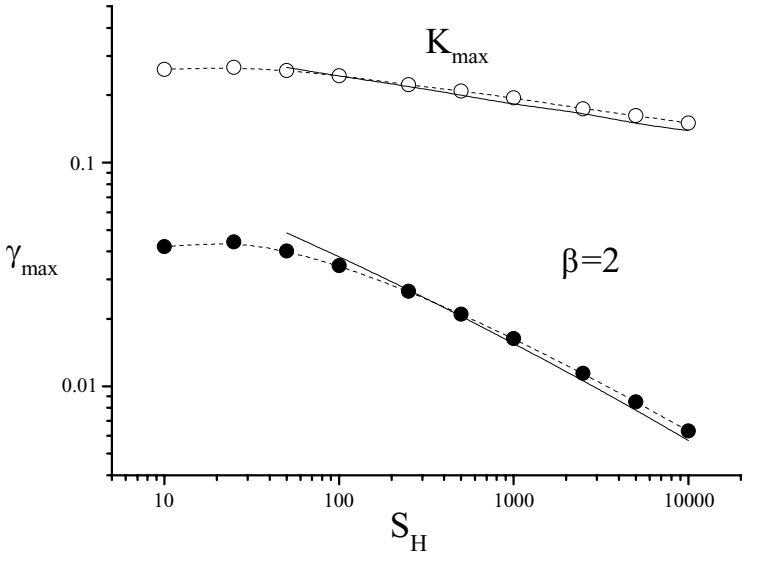

Figure 7. Dependence of the maximum increment and corresponding wave number on Lundquist number for the case of finite $\beta = 2$.

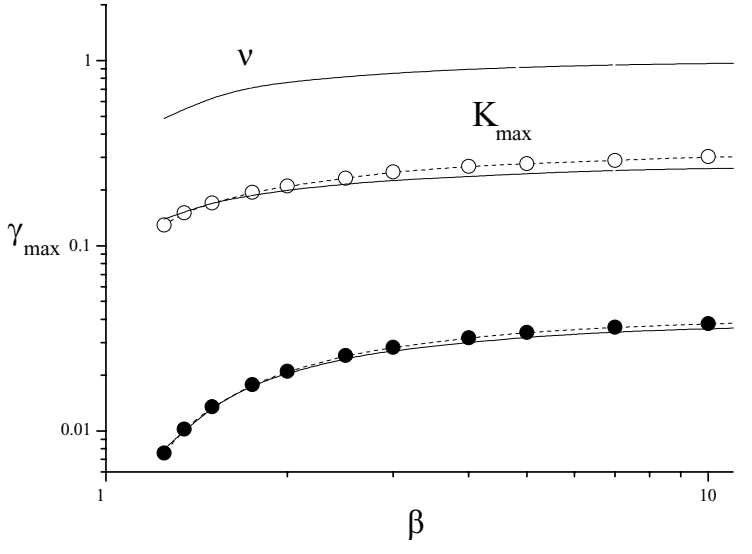

Figure 8. Dependence of the maximum increment and corresponding wave number on beta for Lundquist number $S_{\rm H} = 500$. The function ν given by (23) is also shown.

the case of isotropic resistivity, the following dispersion relation:

$$\alpha \cdot \frac{1+\alpha}{1-\alpha} \cdot \frac{1-\nu+\alpha^2+\sqrt{\alpha+k^2}}{\nu+\alpha^2-\sqrt{\alpha+k^2}} = \frac{1}{\sqrt{S_{\rm H}k}}. \tag{24}$$

Its approximate solution is

$$\gamma_{\max} \approx \frac{\sqrt{1-\nu/3}}{\sqrt{2S_{\rm H}}} \cdot \frac{(2\nu/3)^{2/3}}{1-2\nu/3} \quad \text{at } k_{\max} \approx \frac{\nu/3}{1-\nu/3}. \tag{25}$$

https://doi.org/10.1017/S0022377804002880 Published online by Cambridge University Press

In Fig. 7, the dependence of the maximum increment and corresponding wave number on the Lundquist number is shown at $\beta = 2$. The numerical solution presented for comparison was obtained for a Harris sheet with equilibrium density profile. As one can see, despite quite freehand treatment, the analytical solution shows very good agreement with numerical one. In Fig. 8, the dependence of the increment on β is presented for Lundquist number $S_H = 500$. It might be concluded that the finite β effect substantially reduces growth rate of the tearing instability. For example, it is approximately twice as small at $\beta = 2$ than at $\beta \to \infty$.

5. Conclusion

In the present work, the stability of the neutral current sheet was studied in the frame of Hall dynamics in the plane perpendicular to the main current vector. A new version of resistive tearing instability was found and described. Analytical and numerical solutions of the problem are in satisfactorily agreement and support the validity of each other. It was shown that at sheet width of the order of ion inertia length and even noticeably larger $d \cdot \omega_{pi}/c < \sqrt[3]{S_H}$, Hall rather than ion dynamics determines the diffusion layer and increment. The following properties of instability in the Hall dominated range were found: maximum increment scaling $\gamma \sim S_H^{-1/3}$ is more favorable and the corresponding wave numbers are significantly larger than in the ion-dominated case; in the case of anisotropic resistivity prevailing in the direction of current vector the growth rate is larger; it is strongly reduced by a density ramp at the sheet, the larger the relation n_0/n_∞, the smaller increment. As a whole, inclusion of the Hall term strongly enhances the tearing instability at the ion-inertia range of current sheet widths, especially at very large Lundquist numbers.

Acknowledgement

The author would like to thank Yu. P. Zakharov for numerous and fruitful discussions.

References

[1] Drake, J. F. 2001 *Nature* **410**, 525.
[2] Ma, Z. A. and Bhattacharjee, A. 2001 *J. Geophys. Res.* **106**, 3773.
[3] Yin, L. et al. 2001 *J. Geophys. Res.* **106**, 10761.
[4] Huba, J. D. 1995 *Phys. Plasmas* **2**, 2504.
[5] Carter, T. A. et al. 2000 *Phys. Plasmas* **9**, 3272.
[6] Terasava, T. 1983 *Geophys. Res. Lett.*
[7] Bhattacharjee, A., Ma, Z. W. and Wang, X. 1999 *J. Geophys. Res.* **104**, 14543.
[8] Craig, I. J. D. and Watson, P. G. 2003 *Solar Phys.* **214**, 131.
[9] Priest, E. R. 1985 *Rep. Prog. Phys.* **48**, 1013.